The Activation State of p38 Mitogen-Activated Protein Kinase Determines the Efficiency of ATP Competition for Pyridinylimidazole Inhibitor Binding

Betsy Frantz, Tracey Klatt, Margaret Pang, Janey Parsons, Anna Rolando, Hollis Williams, Michael J. Tocci, Stephen J. O'Keefe, and Edward A. O'Neill*

Department of Inflammation Research, Merck Research Laboratories, Rahway, New Jersey 07065

Received April 13, 1998; Revised Manuscript Received July 27, 1998

ABSTRACT: The serine/threonine kinase p38 is a ubiquitous, highly conserved, stress responsive, signal-transducing enzyme. It regulates the production of proinflammatory mediators and is the target of the cytokine synthesis inhibitory pyridinylimidazoles. We have expressed human p38 in *Drosophila* S2 cells and characterized preparations of mixed unphosphorylated/monophosphorylated (inactive) and homogeneously diphosphorylated (active) forms of the enzyme. We observed that only the active preparation of the enzyme has significant kinase activity when assayed using an ATF2−GST fusion protein as the substrate. We determined that the value of K_M[ATP] in this reaction is 25 μM and that the pyridinylimidazole inhibitor of p38 kinase activity, SB203580, competes with ATP. We have found that a tritiated pyridinylimidazole, SB202190, has an equal affinity for both the active and inactive forms of the enzyme and that SB203580 competes with it equally well for binding to either form of the enzyme. However, ATP can compete with the tritiated inhibitor for binding to only the active form of the enzyme. Further, we demonstrate in vivo that at concentrations consistent with its IC_{50} as a cytokine inhibitor, SB203580 can inhibit stimulus-induced phosphorylation of p38 at the Thr-Gly-Tyr activation motif. Our observations suggest that pyridinylimidazoles may block the biological activity of p38 kinase by binding to the inactive form of p38 and reducing its rate of activation. Under these conditions, ATP would not effectively compete with the inhibitors in vivo.

Small molecule inhibitors of a biological process frequently provide insights into regulatory mechanisms. One such class of molecules, the pyridinylimidazoles, was shown to inhibit proinflammatory cytokine synthesis and has implicated the SAPK[1] p38α as a necessary component in signal transduction pathways leading to secretion of IL-1 and TNFα (*1*). Molecules of this class, typified by SB203580, exhibit a strong correlation between the extent of in vitro p38 binding and in vivo cytokine synthesis inhibition (*1*). Protein kinase inhibitors such as these, both selective and potent in vivo, are exceedingly rare, and the mechanism of action of this class of molecules is of great interest.

The p38α kinase belongs to the family of MAP kinases including p38s β and γ (*1*−*5*), JNKs −1, −2, and −3 (*6*−*8*), and ERKs −1 and −2 (*9*, *10*). All members of this family of kinases are activated by phosphorylation of the Thr and Tyr in a conserved Thr-X-Tyr motif (*11*−*15*).

Recently, three-dimensional structures of nonphosphorylated (inactive) p38α were reported (*16*, *17*). Like numerous other protein kinases whose structures have been solved (see ref *18* for review), p38α contains two distinct domains, one derived largely from the N-terminal portion of the protein and the other from the C-terminal portion. In kinases whose structures have been solved with ATP bound, the N-terminal domain forms a binding site for the adenine ring of ATP and the C-terminal domain provides the binding site for the β-phosphate of ATP, the catalytic base, and the magnesium binding sites. Together, the domains form a catalytic pocket capable of binding all substrates in the proper orientation. However, in the structure of the unphosphorylated form of p38, the N-terminal and C-terminal domains of the enzyme are misaligned. As a result, two residues that interact directly with the β-phosphate of ATP in the cAPK crystal structure (Lys^{53} and Asp^{168}) and which therefore would be predicted to do the same in p38 are further apart in p38 than in cAPK (*19*). Thus, the structure of unphosphorylated p38 may be suboptimal for ATP binding. This analysis suggests that the regulation of p38 kinase activity can be explained by the inability of unphosphorylated p38 to bind ATP tightly. As yet, however, there are no experimental data confirming these structure-based predictions.

Pyridinylimidazole inhibitors of p38 kinase activity, which block proinflammatory cytokine synthesis in a variety of cell types (*1*), are reported to compete with ATP (*20*). Despite the structural features of the unphosphorylated form of p38 described above, which might reduce the extent of ATP binding, a crystal structure of the complex of unphosphorylated p38 and SB203580 has been solved, demonstrating the inhibitor bound in a portion of the ATP pocket of the enzyme (*21*). The bound inhibitor interacts with several sites

* To whom correspondence should be addressed at Merck Research Laboratories, P.O. Box 2000, Building 80M-123, Rahway, NJ 07065. Phone: (732) 594-5313. Fax: (732) 594-1051. E-mail: edward_oneill@merck.com.

[1] Abbreviations: SAPK, stress-activated protein kinase; IL-1, interleukin-1; TNFα, tumor necrosis factor α; cAPK, cAMP-dependent protein kinase; MAPK, mitogen-activated protein kinase; rhp38, recombinant FLAG-tagged human p38α kinase; CSBP, cytokine-suppressive antiinflammatory drug binding protein.

S0006-2960(98)00832-0 CCC: $15.00
Published on Web 09/09/1998

on the enzyme that are predicted to interact with ATP; the pyridyl ring, the imidazole ring, and the *p*-methylsulfinylphenyl group of the inhibitor overlap the corresponding binding sites of the six-membered ring of the adenine, the five-membered ring of adenine, and the phosphate groups of ATP, respectively. The 4-phenyl ring of the inhibitor has no counterpart in ATP and occupies a unique location in the enyme, perhaps contributing to inhibitor selectivity, or to other, inhibitor-specific binding properties (see below).

The subdomain structures of the free and inhibitor-bound forms of p38 are similar, but differences involving the orientations of the N- and C-terminal domains are apparent. As detailed above, the orientation of these domains in free, unphosphorylated p38 is incompatible with tight ATP binding. However, the orientation of the two domains in the structure of inhibitor-bound, unphosphorylated p38 is similar to that of unphosphorylated ERK2 (*19*), which is capable of binding ATP. Thus, it appears that the inhibitor stabilizes a structure of p38 that is compatible with its binding. ATP might accomplish a similar structural stabilization, but there are no reports of ATP-bound, unphosphoryated p38.

If a pyridinylimidazole inhibitor of p38 is capable of high-affinity binding to the unphosphorylated p38 and ATP is not, the inhibitor would have an unexpected thermodynamic advantage in vivo where the high ATP concentration would require very high inhibitor concentrations to effectively compete with ATP. To test this possibility, we have cloned human p38α and expressed it in both a mixed unphosphorylated/monophosphorylated (inactive) form and a diphosphorylated (active) form. With these recombinant proteins and a direct inhibitor binding assay, we demonstrated that a radiolabeled pyridinylimidazole p38 inhibitor (SB202190) can bind both inactive and active forms of the kinase equally well and that SB203580 can compete with this ligand for binding to either form of the enzyme. Further, while binding of the inhibitor to the active form of the enzyme is competitively inhibited by ATP, binding of the inhibitor to the inactive form of the enzyme is unaffected by ATP. Finally, we demonstrate that SB203580 inhibits stimulus induced activating phosphorylation of p38. These data suggest a unique mechanism by which a kinase inhibitor that competes with ATP can function in vivo at concentrations approximately equal to its value of K_i: by binding to a form of the enzyme that is inaccessible to ATP and preventing its transformation to the ATP accessible form of the enzyme.

MATERIALS AND METHODS

Protein Expression and Purification. Expression and purification of recombinant human p38α and ATF2−GST have been described (*22*).

Myelin basic protein (MBP) was purchased from Gibco/BRL.

The protein concentration of recombinant human p38 was calculated with the formula $(1.45OD_{280} - 0.74OD_{260}) \times 0.5$ = milligrams of protein per milliliter (*23*), 0.5 being a p38-specific correction factor established by amino acid analysis.

Amino Acid Analysis. The protein concentration of rhp38 was determined for several independent preparations by amino acid analysis. These preparations were used to standardize quantitation by UV absorbance. Aliquots of the protein (10 μg) were dried in 6 × 50 Pyrex tubes placed in a hydrolysis vial obtained from Pierce Chemical Co. After the vial was dried, 6 N HCl (300 μL) containing 1% phenol was added to the vial, and the vial was degassed for 3 × 90 s while repeatedly flushing with nitrogen. Vapor phase hydrolysis was performed by heating the hydrolysis vial at 120 °C for 18 h. The tubes were dried in vacuo. Beckman's sample buffer (150 μL) was added to the tubes, and after the tubes were vortexed, samples were centrifuged in a benchtop microfuge. Fifty microliters of the sample was analyzed on a Beckman 6300 High Performance Amino Acid Analyzer. A standard solution of amino acids with a known concentration was used to calibrate the instrument. The concentration of the unknown samples was determined on the basis of the calibration standards.

Mammalian Tissue Culture. THP-1 cells were maintained at densities between 2.5×10^5 and 1×10^6 cells/mL in Iscove's Modified Dulbecco's Medium supplemented with L-glutamine, 25 mM Hepes, 1% penicillin/streptomycin, and 10% fetal bovine serum. LPS (Re595) was obtained from Sigma and used at a concentration of 100 ng/mL. Human TNF-α was obtained from Upstate Biotechnology and used at a concentration of 20 ng/mL.

Western Blots. To visualize recombinant, human p38 produced in *Drosophila* S2 cells, extracts were fractionated by SDS−PAGE (12% minigel, Novex), transferred to Immobilon-P (Millipore), and probed with rabbit polyclonal anti-p38(C-20) antibody (Santa Cruz Biotechnology), murine monoclonal anti-FLAG M2 (Kodak) antibody, or rabbit polyclonal phospho-specific p38 MAPK(Tyr182) antibody (New England Biolabs). To visualize native human p38, 2×10^6 THP-1 cells were lysed in buffer containing 20 mM Tris (pH 7.5)/120 mM NaCl/1% Triton X-100/1 mM EDTA/20 mM NaF/2 mM Na_3VO_4/"Complete" protease inhibitor cocktail (Boehringer Mannheim). Lysate was cleared by centrifugation for 10 min at 1400 rpm in an Eppendorf microcentrifuge. The supernatant (cytoplasmic extract) was fractionated by SDS−polyacrylamide gel electrophoresis and processed as above. The fractionated and transferred extract was probed with rabbit polyclonal anti-p38(C-20) antibody to visualize total p38, and rabbit polyclonal anti-phospho-p38(Thr^{180}/Tyr^{182}) antibody (New England Biolabs) to visualize activated p38. In all cases, secondary, horseradish peroxidase-conjugated antibodies were from Amersham and the immune complexes were detected by enhanced chemiluminescence.

Mass Spectroscopy. Mass spectral analysis was performed on a Finnigan MAT TSQ700 triple-quadrupole mass spectrometer equipped with an Applied Biosystems 130 HPLC system. Aliquots of affinity-purified recombinant p38 were injected onto a 2.1 mm × 100 mm C4 reversed phase column and eluted with a linear gradient of 10 to 80% acetonitrile in aqueous 0.085% TFA over a period of 30 min. Aquisition of mass spectral data was initiated 5−10 min after injection and continued for the remainder of the LC run. The p38 protein eluted off the column at approximately 50−55% acetonitrile. Typically, 50−200 pmol of protein was analyzed.

Kinase Assay. The standard p38 kinase assays were performed in a reaction volume of 100 μL, at 30 °C over a period of 20 min under the following conditions: 25 μM Hepes (pH 7.4), 10 mM $MgCl_2$, 0.1 mM Na_3VO_4, 20 mM

β-glycerophosphate, 2 mM DTT, 5 μM ATP, and 10 μCi of [γ-^{33}P]ATP. SB203580 was added to each reaction mixture in 2 μL of DMSO. A time course for each preparation of enzyme was performed to ensure that reaction conditions were within the linear range. For quantitation, the reaction (volume of 100 μL) was terminated with an equal volume of filter-binding stop solution (100 mM EDTA and 15 mM sodium pyrophosphate). Phosphocellulose filter plates (from Millipore) were prewet with filter-binding stop solution; 50 μL aliquots from a single reaction were applied in triplicate to the filter under vacuum, and the filter was subsequently washed three times with 75 mM phosphoric acid. The filters were counted in a Hewlett-Packard Top Count instrument, and the average of the triplicates was determined. The moles of phosphate incorporated were calculated by dividing the counts retained on the filter by the total counts in each reaction multipled by the moles of total ATP in each reaction.

For gel kinase assays, the kinase reactions were terminated by immediately boiling in SDS loading buffer. Reaction products were separated by SDS−PAGE (12% minigel, Novex); the gel was dried, and results of the reaction were visualized and quantitated with a Molecular Dynamics Phosphoimager (model 400E).

Inhibitor Binding Assay. The inhibitor binding assay was modified from a previously described method (*1*). The binding buffer is identical to the kinase reaction buffer described above. [2,6-^{3}H]SB202190 [4-(4-fluorophenyl)-2-(4-hydroxyphenyl)-5-(4-pyridyl)imidazole (71.4 mCi/mg) (*1*)] was mixed with the indicated amounts of immunoaffinity-purified rhp38 in the presence of 200 μg of ATF2−GST in a volume of 100 μL. The binding assay mixture was incubated for 15−30 min at 30 °C, and then a 50 μL portion was loaded onto a small gel filtration column (Centri-Sep, CS-901, Princeton Separations, Princeton, NJ) which had been prepared according to the manufacturer's instructions using elution buffer [20 mM Tris (pH 7.4) and 50 mM 2-mercaptoethanol] to hydrate the column. Inhibitor bound to p38 was separated from free inhibitor by centrifugation of the column for 2 min at 514*g* in a Beckman Model GPR tabletop centrifuge. The entire eluate was collected, mixed with 5 mL of Aquasol-2 scintillation fluid (Packard), and counted in a Beckman LS6000TA scintillation counter. The radioactive material found in the column eluate from a binding assay containing p38 minus that found in the eluate from an identical assay without p38 was taken to represent the amount of inhibitor molecules that were bound specifically to p38. This p38-associated radioactive material binding activity was saturable and could be completely displaced by nonradioactive SB202190 as well as by SB203580 [4-(4-fluorophenyl)-2-[4-(methylsulfinyl)phenyl]-5-(4-pyridyl)imidazole].

RESULTS

Expression and Activation of Recombinant Human p38. A cDNA encoding p38α (CSBP2) (*1*, *2*) was generated from human T cell RNA and modified to encode a protein with an N-terminal FLAG epitope (FLAG-p38). A clonal line of *Drosophila* Schneider cells capable of expressing FLAG-p38 cDNA under control of a copper inducible metallothionein promoter was established (p38-S2). A commercially available polyclonal antiserum raised against a peptide mapping to the carboxyl terminus of p38 recognizes the native enzyme in control mammalian cell extracts (Figure 1A, lane 2). This antiserum was used to detect recombinant FLAG-tagged enzyme in lysates from $CuSO_4$-treated p38-S2 cells (Figure 1A, lanes 3 and 4). Monoclonal M2 antibody directed against the FLAG epitope reacts with a protein with the identical molecular weight (Figure 1A, lanes 6 and 7) in the same lysates. No protein was detected with the M2 antibody in lysates from nontransfected, $CuSO_4$-treated S2 cells (Figure 1A, lane 5).

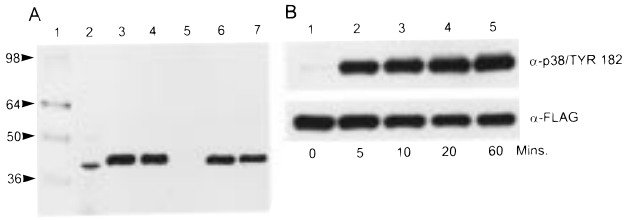

FIGURE 1: Expression and phosphorylation of recombinant human p38α in *Drosophila* S2 cells. (A) Extracts from p38-S2 were generated after induction for 4 h with 1 mM $CuSO_4$. The extracts were fractionated by SDS−polyacrylamide gel electrophoresis, then transferred to Immobilon P membrane, and probed either with polyclonal antiserum raised against a C-terminal peptide of p38 (lanes 3 and 4) or with the anti-FLAG monoclonal antibody M2 (lanes 6 and 7). Lane 1 contained molecular weight markers (as indicated by arrows), lane 2 the C-6 glioma cell extract probed with anti-p38 antiserum, and lane 5 the extract from untransfected S2 cells induced with $CuSO_4$ and probed with anti-FLAG antibody. (B) Extracts from p38-S2 were generated after induction for 4 h with 1 mM $CuSO_4$ and then treatment for varying lengths of time with 400 mM NaCl, 2 mM sodium vanadate, and 100 μg/L okadaic acid. The extracts were fractionated by SDS−polyacrylamide gel electrophoresis, then transferred to Immobilon P membrane, and probed with either phospho-specific p38 MAPK (Tyr^{182}) polyclonal antiserum or the anti-FLAG monoclonal antibody M2, as indicated. Lane 1 contained the extract from cells that were not treated with NaCl, and lanes 2−5 contained extracts from cells that were treated with NaCl for the times indicated above each lane.

In yeast or mammalian cells, p38 can be activated by osmotic shock (*2*, *24*). The enzyme activity results from phosphorylation of p38 on Thr^{180} and Tyr^{182} (*2*, *25*, *26*). Thus, the level of p38 tyrosine phosphorylation can be considered an indicator of enzyme activation. We tested the ability of a combination of 400 mM NaCl, 2 mM Na_3VO_4, and 100 μg/L okadaic acid to induce tyrosine phosphorylation of recombinant human p38 (rhp38) in *Drosophila* S2 cells. We used a commercially available phospho-specific p38 MAPK (Tyr^{182}) antibody to rapidly assess the phosphorylation state of the enzyme at various times after stimulation (Figure 1B). A low level of constitutive tyrosine phosphorylation of rhp38 was observed in lysates from $CuSO_4$-treated cells, and a 5 min stimulation increased the extent of tyrosine phosphorylation of the enzyme dramatically. No further change in phosphorylation level was observed out to 60 min after osmotic shock. We routinely used a 10 min osmotic shock to activate rhp38 prior to purification of the enzyme.

Purification and Characterization of Recombinant Human p38. Rhp38 expressed by $CuSO_4$-treated S2 cells was purified by immunoaffinity chromatography using anti-FLAG agarose (Figure 2, lanes 2 and 3). Preparations of rhp38 were estimated by liquid chromatography−mass spectroscopy to be approximately 90% pure. Liquid chromotography−electrospray mass spectroscopy was also used to

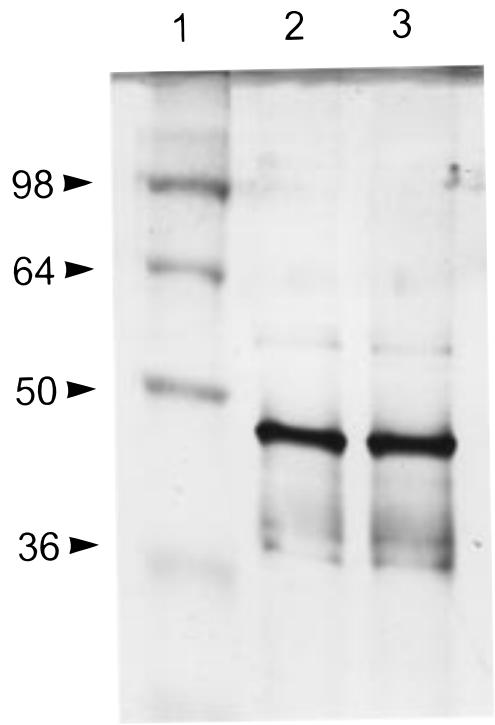

FIGURE 2: Purity of immunoaffinity-chromatographed recombinant human p38. Extracts from p38-S2 were generated after induction for 4 h with 1 mM $CuSO_4$. The extracts were fractionated by chromatography on a column containing anti-FLAG M2 resin. Peptide eluates from the column were fractionated by SDS−polyacrylamide gel electrophoresis, and the gel was silver stained (Daiichi). Lane 1 contained molecular weight markers as indicated by arrows, lane 2 the eluate generated from extracts of cells that had not been osmotically shocked, and lane 3 the eluate generated from extracts of cells that had been osmotically shocked.

evaluate the phosphorylation state of purified recombinant p38 (Figure 3). The majority of the purified protein from $CuSO_4$-induced p38-S2 cells has a molecular weight of 42 345 which is 57 mass units greater than that predicted for rhp38 (Figure 3A). The extra 57 mass units likely results from an unexpected modification of the recombinant protein. Consistent with this interpretation, attempts to sequence the rhp38 demonstrated that the amino terminus of the purified protein was blocked (data not shown). Approximately 30% of the protein has a molecular mass of 42 428 (Figure 3A). This species likely represents a monophosphorylated form of rhp38. Immunoaffinity-purified rhp38 produced by $CuSO_4$-induced osmotically shocked p38-S2 cells has a molecular weight of 42 500 (Figure 3B). This molecular weight is consistent with a diphosphorylated species of the recombinant enzyme. To demonstrate the ability of the mass spectrometer to distinguish between these presumed phosphorylation states of rhp38, we mixed equal portions of protein from the two different preparations. The mass spectrum of this mixture was a near perfect overlay of the two spectra obtained separately (Figure 3C).

Bacterially produced ATF2−GST, reported to be a preferred substrate of p38 (*27*), was used to characterize the activity of immunoaffinity-purified rhp38. To estimate how much of the rhp38 kinase activity obtained from osmotically shocked p38-S2 cells results from dual phosphorylation of rhp38, we compared it with the kinase activity associated with the rhp38 obtained from $CuSO_4$-induced p38-S2 cells that were not osmotically shocked. The rhp38 from unshocked cells exhibits less than 0.1% of the ATF2−GST kinase activity associated with rhp38 from osmotically shocked cells (Figure 4). A gel-based p38 kinase assay was used to demonstrate that only ATF2−GST was phosphorylated in the reaction (Figure 5). The molecular weight of the phosphorylated protein is consistent with the input substrate: approximately 16 000 when MBP is used as the substrate (Figure 5, lanes 2 and 3) and approximately 45 000 when ATF2−GST is used as the substrate (Figure 5, lanes 4 and 5). In either case, the activity of enzyme obtained from osmotically shocked S2 cells was inhibited by SB203580 (Figure 5, lane 2 vs 3 and lane 4 vs 5).

Kinetic Mechanism of Pyridinylimidazole Inhibition. The kinetic constants for p38 using 10 nM enzyme, under conditions where the rate of ATF2−GST phosphorylation was linear with respect to time, were determined. When [ATF2−GST] = 10 μM, the value of K_M^{app}[ATP] = 25 ± 5 μM (data not shown). When [ATP] = 100 μM, the value of K_M^{app} for the GST−ATF2 substrate was 2 ± 1 μM (data not shown). The effect of SB203580 on the rates of p38-catalyzed reactions with respect to ATP was examined at [ATF2−GST] = 10 μM (Figure 6). Reciprocal plots of initial velocities with respect to the concentration of ATP at different fixed concentrations of SB203580 intersected on the 1/*V* axis, confirming that SB203580 behaves as a competitive inhibitor with respect to ATP as previously reported (*20*, *22*).

Analysis of Pyridinylimidazole−ATP−p38 Interaction by a Competitive Drug Binding Assay. To determine the nature of the inhibitor−p38 interactions, we used a binding assay similar to that previously described (*1*). Enzyme was prepared from $CuSO_4$-treated p38-S2 cells (nonactivated p38) or from osmotically shocked $CuSO_4$-treated p38-S2 cells (activated p38). The tritiated form of a p38 inhibitor (SB202190) (*1*) was used as the ligand. Scatchard plots of data derived from SB202190 titrations indicated that the ligand bound equally well to both nonactivated (K_d = 37 nM) and activated (K_d = 38 nM) p38 (Figure 7A,B). The specific binding activities of the nonactivated and activated preparations of rhp38 were virtually identical (Figure 7C), indicating that in the nonactivated preparation both nonphosphorylated and monophosphorylated forms of the enzyme were binding to the inhibitor. We observed a maximum of 50−60% of input ligand bound in this assay (Figure 7C), probably due to ligand−enzyme dissociation that occurs during the separation of the bound and free ligand. The tritiated ligand could be effectively displaced from either nonactivated or activated p38 with either unlabeled self (data not shown) or SB203580 (Figure 7D).

We have previously demonstrated the ability of ATP to compete with SB202190 for binding to activated rhp38 (*22*). With the preparations of enzyme characterized herein, we used the competitive binding assay to compare the ability of ATP to compete with SB202190 for binding to the different forms of rhp38 (Figure 8). At [ATP] = 1 mM (approximately 40 times its K_M in the kinase reaction), only about 10% of the labeled compound remains bound to activated p38. However, at this same high concentration, ATP had no effect on the binding of the compound to nonactivated p38. We interpret these results to indicate that in solution and at physiologically relevant concentrations, ATP cannot compete with this class of pyridinylimidazole

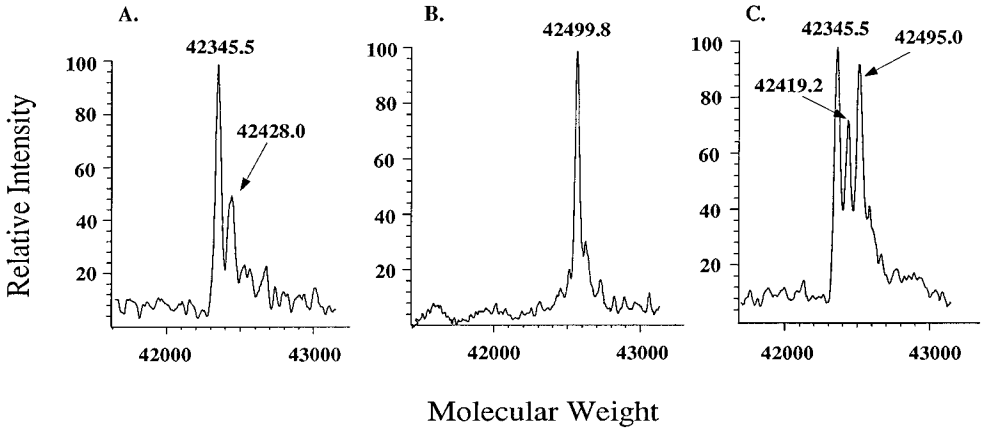

FIGURE 3: Molecular weights of recombinant human p38 from p38-S2 cells. Approximately 50 pmol of each of the immunoaffinity-purified preparations of p38 described in Figure 2 was characterized by LC−MS as described in Materials and Methods: (A) mass spectrum of rhp38 from p38-S2 cells that were not osmotically shocked, (B) mass spectrum of rhp38 from p38-S2 cells that were osmotically shocked, and (C) mass spectrum of mixed rhp38 from both untreated and osmotically shocked p38-S2 cells.

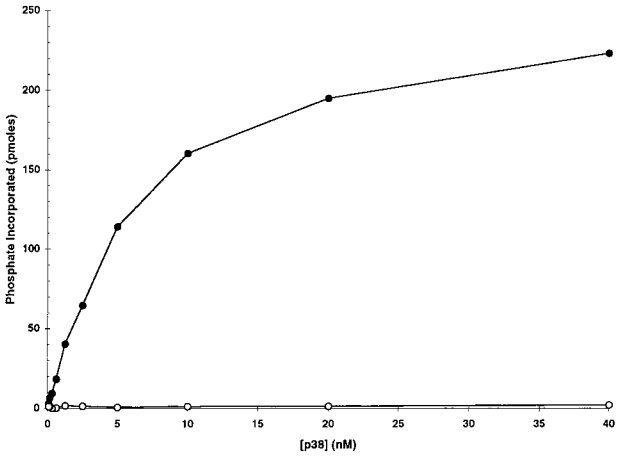

FIGURE 4: Activation of recombinant human p38. The p38-S2 cells were induced with $CuSO_4$ for 4 h and then either collected immediately or osmotically shocked and then collected. Recombinant human p38 was immunoaffinity-purified from each of these sets of cells. The kinase activity of these preparations of rhp38 is presented as picomoles of PO_4 associated with the ATF2−GST substrate in a 30 min reaction: kinase activity from untreated cells (○) and kinase activity from osmotically shocked cells (●).

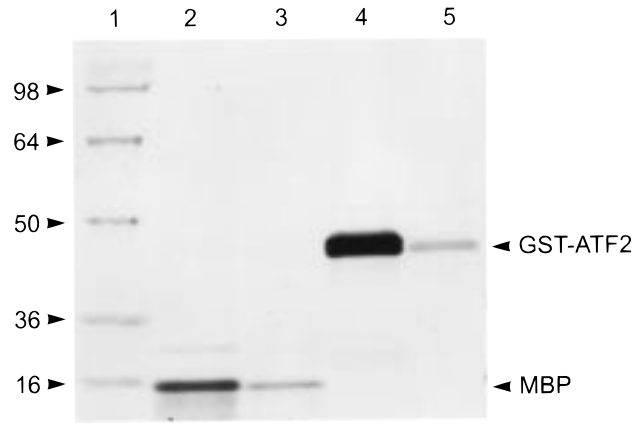

FIGURE 5: Inhibitor sensitivity of recombinant human p38. A culture of p38-S2 cells was induced with $CuSO_4$ for 4 h and then osmotically shocked. Recombinant human p38 was immunoaffinity-purified from these cells. The kinase activity of this preparation of p38 was tested in reaction mixtures containing 10 μg of MBP (lanes 2 and 3) or 5 μg of ATF2−GST (lanes 4 and 5) in the absence of inhibitor (lanes 2 and 4) or in the presence of 30 μM SB203580 (lanes 3 and 5). Lane 1 contained molecular weight markers as indicated by the arrows.

p38 inhibitors for binding to the non- or monophosphorylated forms of p38.

Analysis of SB203580−p38 Interactions in Vivo. If SB203580 binds the inactive form of p38 in vivo, as well as in vitro, it might affect the kinetics of p38 phosphorylation. To test this possibility, we stimulated THP-1 cells with LPS or TNF in the presence of SB203580 at increasing concentrations (Figure 9). The compound inhibits the stimulus-induced phosphorylation of p38 at concentrations precisely consistent with its IC_{50} as an inhibitor of cytokine synthesis.

DISCUSSION

The number of kinases regulated via dual phosphorylation of a Thr-X-Tyr motif and their evolutionary conservation demonstrate the utility and versatility of this regulatory mechanism (*24*). In addition, some of the biological events controlled by Thr-X-Tyr-regulated kinases have been implicated in pathological conditions (*1*), indicating that these kinases may be targets for therapeutic intervention. Therefore, understanding the mechanism by which known inhibitors of these kinases function could prove useful in developing novel pharmacological agents.

In this report, we describe the biochemical and enzymological characterization of recombinant human p38 produced in *Drosophila* S2 cells. Our first observation, that osmotic shock results in the phosphorylation and activation of human p38 in insect cells, demonstrates the evolutionary conservation of this signal transduction pathway.

A class of compounds whose members inhibit p38s α and β has been used to define the critical role these enzymes play in regulating both the synthesis of and responses to IL-1 and TNF (*1*). We have determined that while these compounds compete with ATP to inhibit p38 kinase activity, they are capable of binding to inactive p38 in a manner that is not competitive with ATP.

As a first step toward determining the mechanism by which the pyridinylimidazole class of inhibitors blocks p38 kinase activity, we determined the Michaelis constants for the substrates of a p38-mediated kinase reaction. As reported (*27*), bacterially produced ATF2−GST serves as an efficient protein substrate for recombinant p38 (Figure 4). We

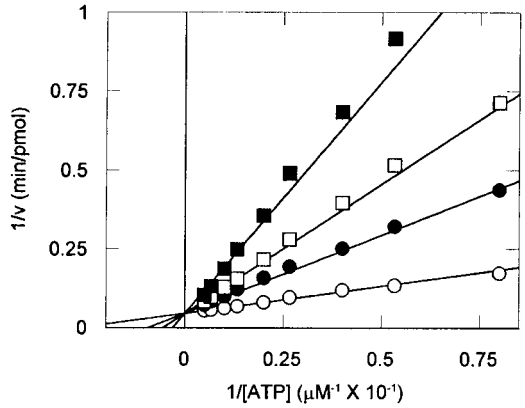

FIGURE 6: Kinetic analysis of the nature of p38 inhibition by a triarylimidazole. Standard kinase reactions with 10 nM diphosphorylated p38 and ATP at varying concentrations as indicated without (○) or with 50 (●), 100 (□), or 200 (■) nM SB203580 were carried out for 20 min at 30 °C. Kinetic parameters were determined using a nonlinear least-squares fit of the [S]−v data to the competitive inhibition rate equation (GraFit 3.5, Erithacus Software Ltd., Staines, U.K.). The graph shows a double-reciprocal plot of the fit data.

determined a value for K_M^{app}[ATF2−GST] of 2 ± 1 μM. This value is consistent with the previously reported values of K_M^{app} for protein substrates of other MAPK family members (*28*). K_M^{app}[ATP] = 25 ± 5 μM in the p38-mediated reaction. This value is within the expected range based on previously examined protein kinases (*29*) but is 10-fold lower than that recently reported by Young et al. (*20*). Young et al. measured the value of K_M^{app}[ATP] using the epidermal growth factor receptor-derived peptide (T699), while we used a fusion protein derived from the transcription factor ATF-2. The difference in the values of the apparent K_M is likely due to the use of different phosphate acceptors and might reflect the contributions a protein substrate can make to ATP binding affinity. This effect of protein substrate on the value of K_M^{app}[ATP] is consistent with the recently proposed mechanism for p38, ordered sequential with protein substrate binding before ATP (*22*). Having established the kinetic constants associated with our standard kinase reaction, we were able to demonstrate that the pyridinylimidazole SB203580 is a competitive inhibitor of ATP binding to p38 kinase (Figure 6).

To assess how well the inhibitor binds to the nonactivated form of the enzyme, we immunoaffinity purified recombinant p38 from S2 cells that had not been treated with 400 mM NaCl. We observed that tritiated SB202190 could bind to both the inactive and the active forms of the enzyme (Figure 7A,B). The values of K_d for the complex between the inhibitor and either form of the recombinant enzyme (approximately 37 nM) in our binding assay are similar to published data for the native protein (30−50 nM) (*1*). We also demonstrated that SB203580, the pyridinylimidazole molecule most commonly used, competes effectively with the labeled molecule for binding to either form of the enzyme

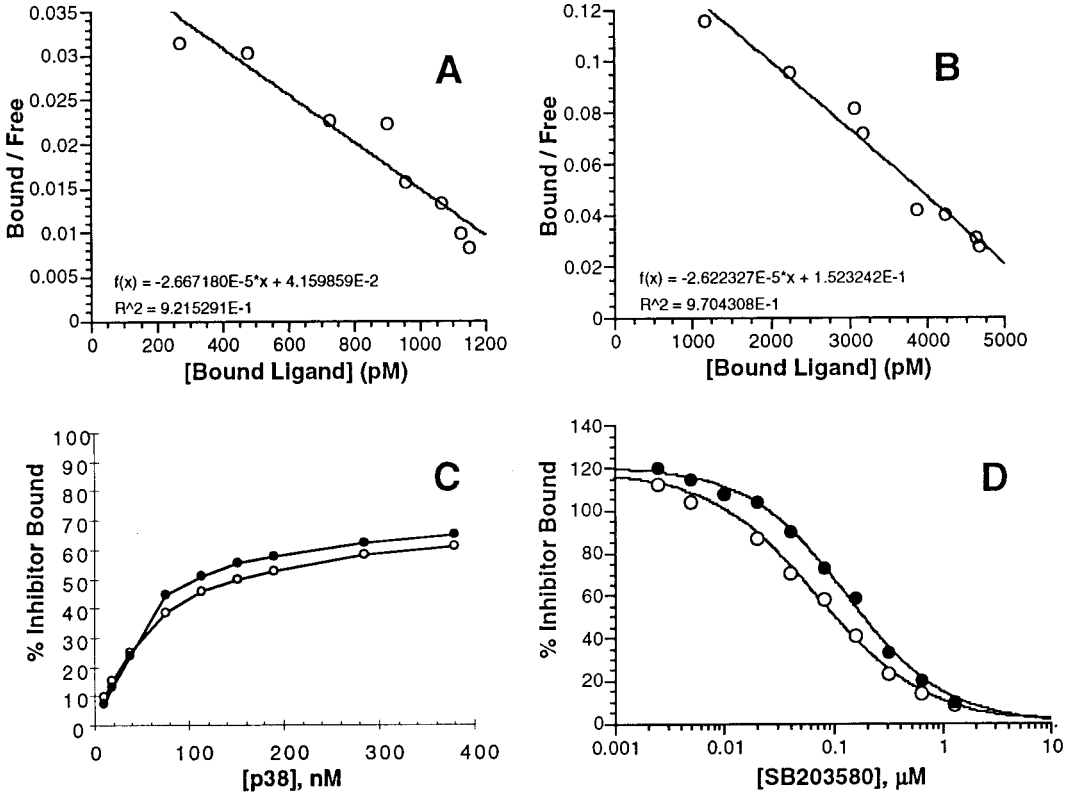

FIGURE 7: Determination of the affinity between inhibitors of p38 and differently phosphorylated species of p38. (A and B) Increasing concentrations of [2,6-^{3}H]SB202190 were incubated with 4.8 nM p38 isolated from untreated p38-S2 cells (A) or 8 nM p38 from cells that had been osmotically shocked prior to harvesting (B). The amount of free inhibitor was calculated as the difference between the amounts of bound inhibitor and total inhibitor in the binding assay. The data points were fit to a line with DeltaGraph (Delta Point, Inc., Monterey, CA), and the value of K_d was calculated as the negative reciprocal of the slope term in the formula defining each line. (C) Increasing concentrations of rhp38 isolated from $CuSO_4$-induced S2 cells that were untreated (○) or from cells that had been osmotically shocked (●) were incubated with 25 nM [2,6-^{3}H]SB202190. (D) [2,6-^{3}H]SB202190 (12.5 nM) and SB203580 at the indicated concentrations were incubated with 24 nM p38 isolated from untreated p38-S2 cells (○) or 25 nM p38 from cells that had been osmotically shocked prior to harvesting (●). In all cases, protein−inhibitor complexes were separated from free inhibitor as described in Materials and Methods.

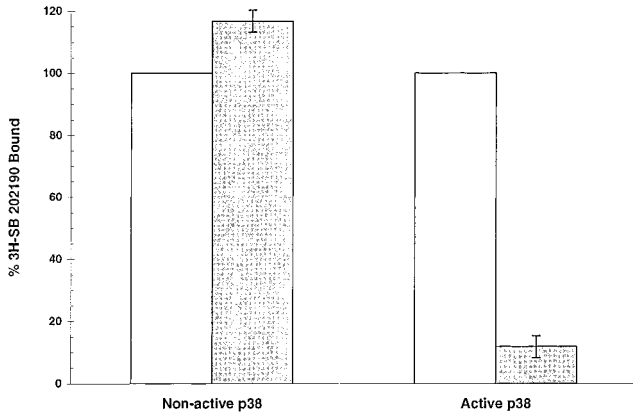

FIGURE 8: Competitive binding assay measuring the interaction between p38 and ATP. [2,6-^{3}H]SB202190 (12.5 nM) was incubated with 19 nM p38 isolated from $CuSO_4$-induced p38-S2 cells that were untreated (inactive p38) or 8 nM p38 from cells that had been osmotically shocked prior to harvesting (active p38), in the absence (white bars) or presence (shaded bars) of 1 mM ATP. The amount of protein−inhibitor complex was quantitated as described in Materials and Methods. The amount of complex formed in each case in the absence of ATP was set to 100%.

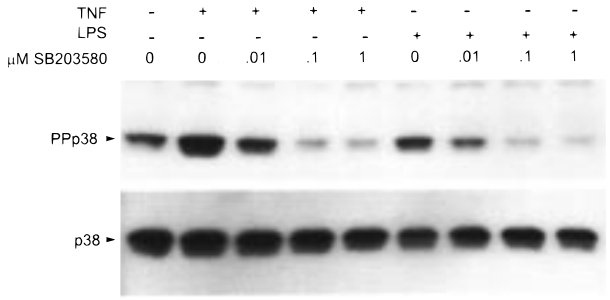

FIGURE 9: Effect of SB203580 on phosphorylation at Thr-Gly-Tyr of p38 in vivo. Cytoplasmic extracts of THP-1 cells that were untreated or treated with bacterial LPS or human TNF-α for 20 min, in the absence or presence of the indicated concentration of SB203580, were fractionated by electrophoresis on a 12% SDS−polyacrylamide gel, transferred by electrophoresis to Immobilon P membrane, and probed with anti-p38 (p38) or anti-phospho(Thr^{180}/Tyr^{182})-p38 (PPp38).

(Figure 7D). Finally, we used the binding assay to demonstrate that activation of the enzyme results in a conformation which allows ATP to compete with the inhibitor for binding. This conformation must be distinct from that of the inactive enzyme since ATP cannot compete with the inhibitor for binding to the nonphosphorylated form. These results are consistent with the predictions from the crystal structure of p38 which demonstrate that in the unphosphorylated state of the enzyme the catalytic residues which would interact with ATP are misaligned (*16*, *17*) but, taken together with the structural analysis of pyridinylimidazole-bound p38 (*21*), suggest that the inhibitor can bind to a conformation of the inactive enzyme that ATP cannot.

Our data, together with the data derived from the crystal structures of ERK2 (*19*) and p38 (*16*, *17*), suggest that at least one aspect of the regulation of ERK2 and p38 by dual phosphorylation might result from different mechanisms. In the case of ERK2, ATP binds unphosphorylated ERK2 and phosphorylation of Thr^{183} and Tyr^{185} causes a change in the phosphoacceptor recognition site and a change in the structure of the catalytic pocket, allowing ATP to achieve an enzymatically productive orientation (*30*). Our data suggest that in contrast with ERK2, ATP binds to the unphosphorylated form of p38 so poorly that at physiological concentrations it is not bound to the enzyme at all. Phosphorylation of p38 at Thr^{180} and Tyr^{182} induces a significant reorientation of the two major domains of p38, aligning several key residues in these domains and significantly increasing its affinity for ATP.

Together, our results suggest two possible mechanisms by which a kinase inhibitor that is competitive with respect to ATP binding can act with the same relative potency in vitro that it does in vivo, in the face of a high in vivo ATP concentration (possibly 100 times its value of K_M^{app}). In either model, the inhibitor binds to a form of the enzyme that is not accessible to the competitor. One model results from the possibility that the inhibitor, once bound to the inactive enzyme, can then stay bound to the enzyme for the duration of the enzyme's active state lifetime, thus inhibiting the enzyme activity despite potential competition with ATP. In vitro, under phosphatase-free conditions, the active state lifetime of the enzyme is virtually infinite, and thus, inhibition by the pyridinylimidazole is strictly competitive with ATP. In vivo, however, activated p38 will be inactivated by cellular phosphatases at some cell- and stimulus-dependent rate. Thus, with an inhibitor with a sufficient affinity and an enzyme active state with a sufficiently short lifetime, the inhibitor would behave as if it were noncompetitive with ATP. To establish the possible relevance of this hypothesis, accurate measurements of both in vitro enzyme−inhibitor complex half-lives and in vivo enzyme active state half-lives will be required.

A second model results from the possibility that the inactive p38−inhibitor complex is a poorer substrate for activating kinases than is inactive p38 alone. Data presented in Figure 9 are consistent with this model. From these data, it appears that pyridinylimidazole inhibitors of p38 kinase may possess a previously undetected activity that makes them uniquely effective in vivo, the ability to bind the inactive form of p38 noncompetitively with ATP and then keep the enzyme in a configuration that cannot bind ATP. Thus, the true activity of these compounds in vivo may be inhibition of p38 activation rather than inhibition of p38 enzymatic activity.

ACKNOWLEDGMENT

We thank Bob Frankshun for synthesis of SB203580 and Linda Chang for synthesis of SB202190.

REFERENCES

1. Lee, J. C., Laydon, J. T., McDonnell, P. C., Gallagher, T. F., Kumar, S., Green, D., McNutly, D., Blumenthal, M., Heys, J. R., Landvatter, S. W., Strickler, J. E., McLaughlin, M. M., Siemens, I. R., Fisher, S. M., Livi, G. P., White, J. R., Adams, J. L., and Young, P. R. (1994) *Nature 372*, 739−746.
2. Han, J., Lee, J.-D., Bibbs, L., and Ulevitch, R. J. (1994) *Science 265*, 808−811.
3. Jiang, Y., Chen, C., Li, Z., Guo, W., Gegner, J. A., Lin, S., and Han, J. (1996) *J. Biol. Chem. 271*, 17920−17926.
4. Lechner, C., Zahalka, M. A., Giot, J.-F., Moller, N. P. H., and Ullrich, A. (1996) *Proc. Natl. Acad. Sci. U.S.A. 93*, 4355−4359.
5. Li, Z., Jiang, Y., Ulevitch, R. J., and Han, J. (1996) *Biochem. Biophys. Res. Commun. 228*, 334−340.

6. Kyriakis, J. M., Banerjee, P., Nikolakakl, E., Dai, T., Ruble, E. A., Ahmad, M. F., Avruch, J., and Woodgett, J. R. (1994) *Nature 369*, 156.
7. Derijard, B., Hibi, M., Wu, I. H., Barrett, T., Su, B., Deng, T., Karin, M., and Davis, R. J. (1994) *Cell 76*, 1025−1037.
8. Gupta, S., Barrett, T., Whitmarsh, A. J., Cavanagh, J., Sluss, H. K., Derijard, B., and Davis, R. J. (1996) *EMBO J. 15*, 2760−2770.
9. Boulton, T. G., Nye, S. H., Robbins, D. J., Ip, N. Y., Radziejewska, E., Morgenbesser, R. A., DePinho, R. A., Panayotatos, N., Cobb, M. H., and Yancopoulos, G. D. (1991) *Cell 65*, 663−675.
10. Seger, R., et al. (1991) *Proc. Natl. Acad. Sci. U.S.A. 88*, 6142−6146.
11. Seger, R., Ahn, N. G., Posada, J., Munar, E. S., Jensen, A. M., Cooper, J. A., Cobb, M. H., and Krebs, E. G. (1992) *J. Biol. Chem. 267*, 14373−14381.
12. Gomez, N., and Cohen, P. (1991) *Nature 353*, 170−173.
13. Anderson, N., Maller, J., Tonks, N. K., and Sturgill, T. W. (1990) *Nature 343*, 651−653.
14. Boulton, T. G., Yancopoulos, G. D., Gregory, J. S., Slaughter, C., Moomaw, C., Hsu, J., and Cobb, M. H. (1990) *Science 249*, 64−67.
15. Payne, D. M., Rossomando, A. J., Erickson, A. K., Her, J.-H., Shabanowitz, J., Hunt, D. F., Weber, M. J., and Sturgill, T. W. (1991) *EMBO J. 10*, 885−892.
16. Wilson, K. P., Fitzgibbon, M. J., Caron, P. R., Griffith, J. P., Chen, W., McCaffrey, P. G., Chambers, S. P., and Su, M. S.-S. (1996) *J. Biol. Chem. 271*, 27696−27700.
17. Wang, Z., Harkins, P. C., Ulevitch, R. J., Han, J., Cobb, M. H., and Goldsmith, E. J. (1997) *Proc. Natl. Acad. Sci. U.S.A. 94*, 2327−2332.
18. Goldsmith, E. J., and Cobb, M. H. (1994) *Curr. Opin. Struct. Biol. 4*, 833−840.
19. Zhang, F., Strand, A., Robbins, D., Cobb, M. H., and Goldsmith, E. J. (1994) *Nature 367*, 704−711.
20. Young, P. R., McLaughlin, M. M., Kumar, S., Kassis, S., Doyle, M. L., McNulty, D., Gallagher, T. F., Fisher, S., McDonnell, P. C., Carr, S. A., Huddleston, M. J., Seibel, G., Porter, T. G., Livi, G. P., Adams, J. L., and Lee, J. C. (1997) *J. Biol. Chem. 272*, 12116−12121.
21. Tong, L., Pav, S., White, D. M., Rogers, S., Crane, K. M., Cywin, C. L., Brown, M. L., and Pargellis, C. A. (1997) *Nat. Struct. Biol. 4*, 311−316.
22. LoGrasso, P. V., Frantz, B., Rolando, A. M., O'Keefe, S. J., Hermes, J. D., and O'Neill, E. A. (1997) *Biochemistry 36* (34), 10422−10427.
23. Kalckar, H. (1947) *J. Biol. Chem. 167*, 461.
24. Waskiewicz, A. J., and Cooper, J. A. (1995) *Curr. Opin. Cell Biol. 7*, 798−805.
25. Derijard, B., Raingeaud, J., Barrett, T., Wu, I. H., Han, J. H., Ulevitch, R. J., and Davis, R. J. (1995) *Science 267*, 682−685.
26. Kumar, S., McLaughlin, M. M., McDonnell, P. C., Lee, J. C., Livi, G. P., and Young, P. R. (1995) *J. Biol. Chem. 270*, 29043−29046.
27. Raingeaud, J., Gupta, S., Rogers, J. S., Dickens, M., Han, J., Ulevitch, R. J., and Davis, R. J. (1995) *J. Biol. Chem. 270*, 7420−7426.
28. Kallunki, T., Su, B., Tsigelny, I., Sluss, H. K., Derijard, B., Moore, G., Davis, R., and Karin, M. (1994) *Genes Dev. 8*, 2996−3007.
29. Force, T., Bonventre, J. V., Heidecker, G., Rapp, U., Avruch, J., and Kyriakis, J. M. (1994) *Proc. Natl. Acad. Sci. U.S.A. 91*, 1270−1274.
30. Canagarajah, B. J., Khokhlatchev, A., Cobb, M. H., and Goldsmith, E. J. (1997) *Cell 90*, 859−869.

BI980832Y